

Global phase and voltage synchronization for power inverters: a decentralized consensus-inspired approach

Marcello Colombino, Dominic Groß, and Florian Dörfler

Abstract—In this work, we explore a new approach to controlling networks of inverters to achieve synchronization of phase angles, frequencies, and ensure convergence to a desired voltage magnitude. We design a synchronizing vector field for a network of interconnected inverters which induces consensus-like dynamics and admits a fully decentralized implementation. We show that the combination of the synchronizing feedback and a simple voltage control law ensures synchronization of the inverters' phase angles and frequencies, as well as convergence of the voltage magnitudes from almost all initial conditions. Furthermore, we show that the controller exhibits a droop-like behavior around the standard operating point thus making it backwards-compatible with the existing power grid.

I. INTRODUCTION

The electric power grid is undergoing a period of unprecedented change. A major transition is the replacement of bulk generation based on synchronous machines by distributed generation interconnected to the grid via power electronics devices fed by renewable energy sources. This gives rise to scenarios in which either parts of the transmission grid or an islanded distribution grid may operate without conventional synchronous generation. In either case, the power grid faces great challenges due to the loss of rotational inertia and the self-synchronizing dynamics of synchronous generators.

The prevalent approaches to controlling inverters as well as to operate the future grid are based on mimicking the physical characteristics and controls of synchronous machines [1]–[3]. On the one hand, this leads to a well-studied closed-loop behavior compatible with the legacy power system. On the other hand, this approach may not be optimal for controlling inverters. In particular, generator-emulation-based strategies use a system with fast actuation but almost no inherent energy storage (the inverter) to mimic a system with slow actuation but significant energy storage (the synchronous generator). Depending on the implementation emulation-based strategies may also be ineffective or result in deteriorating effects due to stringent limits on the tolerable short-circuit currents as well as time-delays in the control loops [4], [5].

In this work, we focus on the problem of ensuring synchronization of a zero-inertia, i.e., generator-free, power

system. This can be part of an islanded transmission grid with high penetration of renewables or a micro-grid operating in islanded mode. The problem of synchronization for power inverters has been extensively studied in the literature. Most of the common approaches study droop control [6], [7] and, for the purpose of analysis, rely on modified versions of the Kuramoto model of coupled oscillators [8]–[10]. While providing useful insights, these approaches often neglect the voltage dynamics, the associated phasor models are well-defined only near the synchronous steady-state, and the synchronization guarantees are only local as the phasor dynamics admit multiple equilibria on the torus. More recent approaches rely on controlling the inverters to behave like virtual Liénard-type oscillators [11]–[16]. This is a promising approach as virtual oscillators can globally synchronize an inverter-based power network and have been validated experimentally. As of today, it is unclear, however, how to build on top of the basic virtual oscillator controller to add secondary regulation loops or to force the network to a desired pre-specified solution of the power flow equations with nonzero relative angles between the voltage vectors.

To overcome these challenges of emulation, droop, and virtual oscillator control, we start from a time-domain model formulated in three-phase current and voltage coordinates. Inspired by consensus strategies [17], [18], we begin by designing fully decentralized controllers making use of only local measurements and local power set-point specifications. Then, we show that the proposed controller, much like virtual oscillators and most generator emulation strategies, behaves similarly to a conventional droop controller around the synchronous harmonic steady state. This salient feature ensures predictable behavior in case of small power imbalances and backward-compatibility with the existing grid. Additionally, in comparison to other control strategies, our decentralized consensus-inspired controller provably asymptotically stabilize prescribed set-points from almost all initial conditions.

Notation

The set of real numbers is denoted by \mathbb{R} . \mathbb{R}_+ denotes the set of nonnegative reals. Given a matrix A , A^\top denotes its transpose. We use $\bar{\sigma}(A)$ to indicate the largest singular value of A . We write $A \succcurlyeq 0$ ($A \succ 0$) to denote that A is symmetric and positive semidefinite (definite). We denote with \otimes the Kronecker product.

Given $\theta \in [0, 2\pi]$ we define

$$R(\theta) := \begin{bmatrix} \cos(\theta) & -\sin(\theta) \\ \sin(\theta) & \cos(\theta) \end{bmatrix} \in \mathbb{R}^{2 \times 2}, \quad J := R(\pi/2).$$

This work was partially funded by the European Union's Horizon 2020 research and innovation programme under grant agreement N° 691800 and the ETH Seed Project SP-ESC 2015-07(4). This article reflects only the authors' views and the European Commission is not responsible for any use that may be made of the information it contains.

The authors are with the Automatic Control Laboratory, ETH Zürich, Switzerland. e-mail: {mcolombi,grodo,dorfler}@control.ee.ethz.ch.

II. MODELING AND CONTROL ARCHITECTURE

In this section we introduce the model of the inverter-based power grid that will be studied throughout the paper.

A. Modeling of inverter-based power grids

We study the control of N three-phase inverters in a low-inertia power system, possibly islanded and without synchronous generators. The inverters are interconnected by a resistive-inductive network with a setup similar to [11]–[16]. Each inverter is abstracted as a controllable voltage source as illustrated in Figure 1. To each inverter we associate a controllable voltage $v_k \in \mathbb{R}^2$ and a measurable output current $i_{o,k} \in \mathbb{R}^2$. All electrical quantities in the three-phase network are assumed to be balanced. This allows us to work in the $\alpha\beta$ coordinate frame using two- instead of three-dimensional vectors for the voltage and current variables by applying the well-known Clarke transformation to the three-phase variables [19].

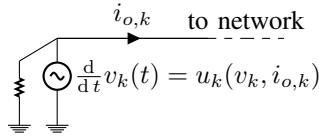


Fig. 1. Schematics of the decentralized control setup: the voltage v_k is fully controllable but only using local measurements.

We model the power grid as an undirected graph $\mathcal{G} = (\mathcal{V}, \mathcal{E}, \mathcal{W})$, where $\mathcal{V} = \{1, \dots, N\}$ is the set of nodes corresponding to the inverters, $\mathcal{E} \subset \mathcal{V} \times \mathcal{V}$, with $|\mathcal{E}| = M$, is the set of undirected edges corresponding to the transmission lines, and \mathcal{W} is the weight matrix with weights w_{jk} defined as

$$w_{jk} := \frac{1}{\sqrt{r_{jk}^2 + \omega_0^2 \ell_{jk}^2}}, \quad (1)$$

where r_{jk} and ℓ_{jk} are respectively the resistance and inductance of the line (j, k) .

If B is the directed incidence matrix of the graph, we define $\mathcal{B} := B \otimes I_2$ that, duplicates each edge for the α and β components. We construct the diagonal matrices $R_T \in \mathbb{R}^{M \times M}$ and $L_T \in \mathbb{R}^{M \times M}$ that contain the values of the resistance and inductance of every line on the main diagonal and the matrices $\mathbf{R}_T := R_T \otimes I_2$ and $\mathbf{L}_T := L_T \otimes I_2$ that duplicate the inductance and resistance values for the α and β components.

We assume that the inverters are controlled such that the time constants of the transmission lines are much faster than those of terminal voltages. We therefore assume that the lines reach steady state almost instantaneously and couple all inverters through the algebraic relationship.¹

$$i_o = \mathcal{Y}v,$$

¹This assumption may be made rigorous using time-scale separation based on singular perturbation analysis but this is beyond the scope of the paper. In Section VI we will show in simulation the effectiveness of the controller taking the line dynamics into consideration.

where $i_o = [i_{o,1}^\top, \dots, i_{o,N}^\top]^\top$, $v = [v_1^\top, \dots, v_N^\top]^\top$ and \mathcal{Y} is the impedance matrix of the network. Using $\mathcal{J} := I_N \otimes J$, the impedance matrix \mathcal{Y} can be constructed as

$$\mathcal{Y} = \mathcal{B}(\mathbf{R}_T + \omega_0 \mathcal{J} \mathbf{L}_T)^{-1} \mathcal{B}^\top. \quad (2)$$

Note that, since $\alpha\beta$ coordinates can be thought as an embedding of the complex numbers into real-valued Euclidean coordinates, the 90° rotation matrix J plays the same role that the imaginary unit $\sqrt{-1}$ plays in complex coordinates.

Note the similarity between the expression of the impedance matrix of the power network (2) and the graph Laplacian matrix

$$L := B \operatorname{diag}(\{w_{jk}\}_{\{j,k\} \in \mathcal{E}}) B^\top. \quad (3)$$

In order to formalize this similarity, let us make the following standard assumption.

Assumption 1 (Uniform inductance-resistance ratio)

The ratio between the inductance and resistance of each transmission line is constant, i.e., there exist $\rho > 0$ so that

$$\frac{\ell_{jk}}{r_{jk}} = \rho, \quad \forall (j, k) \in \mathcal{E}.$$

Assumption 1 is realistic as it means that the transmission lines are constructed with the same material across the network. Let us define the quantity $\kappa := \tan^{-1}(\rho \omega_0)$. Given the power system's graph \mathcal{G} , it is easy to verify that the extended Laplacian $\mathcal{L} := L \otimes I_2$ can be constructed as

$$\mathcal{L} = \mathcal{R}(\kappa) \mathcal{Y}, \quad (4)$$

where $\mathcal{R}(\kappa) = \operatorname{diag}(\{R(\kappa)\}_{i=1}^N)$.

The extended Laplacian \mathcal{L} is equivalent to the Laplacian of a larger graph that presents two identical connected components, one for the α and one for the β coordinate. By using (4) we note that, in order to obtain a Laplacian feedback on the voltages, we can alternatively use a local feedback on the current measurements.

$$\mathcal{R}(\kappa) i_o = \mathcal{L} v. \quad (5)$$

B. Decentralized control of inverter-based power grids

When we control a power inverter, we assume that we can prescribe any dynamics for the terminal voltage that relies only on local measurements. We choose the following controller structure depicted in Figure 1:

$$\frac{d}{dt} v_k = u_k(v_k, i_{o,k}), \quad k \in \mathcal{V}, \quad (6)$$

III. CONTROL OBJECTIVES

The challenge of controlling power inverters as in (6), is that each controller needs to be decentralized, i.e., it can only rely on measurements of the local voltages and currents, while the control objectives are global in nature. Let us begin with a definition of instantaneous active and reactive power

Definition 1 (Instantaneous Power)

Given the AC voltage v_k at a node $k \in \mathcal{V}$ and the AC current $i_{o,k}$ flowing out of the node, we define the corresponding

instantaneous active power $p_k := v_k^\top i_{o,k} \in \mathbb{R}$ and instantaneous reactive power $q_k := v_k^\top J i_{o,k} \in \mathbb{R}$ flowing out of the node.

Active and reactive powers cannot be prescribed arbitrarily to each inverter in a network but they need to be consistent to the power-flow equations [20].

Definition 2 (Consistent set-points)

The set-points p_k^* , q_k^* , v_k^* for active power, reactive power and voltage magnitude respectively, are consistent with the power flow equations if there exist angles θ_{jk}^* such that

$$\begin{aligned} p_k^* &= \sum_{(j,k) \in \mathcal{E}} \frac{v_k^{*2} r_{jk} - v_k^* v_j^* (r_{jk} \cos(\theta_{jk}^*) + \omega_0 \ell_{jk} \sin(\theta_{jk}^*))}{r_{jk}^2 + \omega_0^2 \ell_{jk}^2}, \\ q_k^* &= \sum_{(j,k) \in \mathcal{E}} \frac{v_k^{*2} \omega_0 \ell_{jk} - v_k^* v_j^* (\omega_0 \ell_{jk} \cos(\theta_{jk}^*) - r_{jk} \sin(\theta_{jk}^*))}{r_{jk}^2 + \omega_0^2 \ell_{jk}^2}. \end{aligned} \quad (7)$$

In this work we are interested in designing a controller such that the inverters not only synchronize to a common frequency, but also converge to a desirable solution of the power-flow equations (7). More formally, given power and voltage magnitude set-points p_k^* , q_k^* , v_k^* that are consistent with the power-flow equations according to Definition 2, and a desired synchronous frequency $\omega_0 \geq 0$, we want the closed loop system to satisfy the following objectives:

- **Frequency synchronization:** At steady state all voltage vectors behave like harmonic oscillators with frequency ω_0 i.e.,

$$\lim_{t \rightarrow \infty} \left[\frac{d}{dt} v_k(t) - \omega_0 J v_k(t) \right] = 0, \quad k \in \mathcal{V}. \quad (8)$$

- **Voltage magnitude:** At steady state all voltage vectors have the correct magnitude i.e.,

$$\|v_k\| = v_k^*, \quad k \in \mathcal{V}. \quad (9)$$

- **Power flows:** At steady state, each inverter injects the prescribed active and reactive power i.e.,

$$\begin{cases} v_k^\top i_{o,k} = p_k^* \\ v_k^\top J i_{o,k} = q_k^* \end{cases}, \quad k \in \mathcal{V}. \quad (10)$$

IV. GLOBALLY SYNCHRONIZING DYNAMICS

In this section we introduce the globally synchronizing decentralized controller. In particular we design a vector field of the form (6) that achieves the three objectives (8)-(10) from almost all initial conditions.

A. Decentralized controller

Given power and voltage magnitude set-points p_k^* , q_k^* , v_k^* , we define the matrices

$$K_k := \frac{1}{v_k^{*2}} R(\kappa) \begin{bmatrix} p_k^* & q_k^* \\ -q_k^* & p_k^* \end{bmatrix}. \quad (11)$$

and the nonlinear functions

$$\Phi_k(v_k) := \frac{v_k^* - \|v_k\|}{v_k^*}. \quad (12)$$

We propose the following decentralized control law of the form (6) to achieve the closed-loop objectives (8)-(10):

$$\begin{aligned} \frac{d}{dt} v_k &= u_k(v_k, i_{o,k}) = \\ &\omega_0 J v_k + \eta (K_k v_k - R(\kappa) i_{o,k}) + \alpha \Phi_k(v_k) v_k. \end{aligned} \quad (13)$$

In the remainder of the section we analyze the closed-loop induced by the control law (13). First we show that, in rectangular coordinates, the closed-loop system presents very natural consensus-like dynamics. Next we compare it with existing solutions proposed in the literature. Finally in Section V we will show that (13) indeed synchronizes the power-system to the desired power-flow solution, thus achieving the objectives (8)-(10).

B. Properties of the closed loop

Let us define the block-diagonal matrix $\mathcal{K} := \text{diag}(\{K_k\}_{k=1}^N)$ and the matrix valued function $\Phi(v)$ as

$$\Phi(v) := \text{diag} \left(\{\Phi_k(v_k)\}_{k=1}^N \right). \quad (14)$$

Then, using the relationship (5), we can write the closed loop arising from the controller (13) as

$$\frac{d}{dt} v = \omega_0 \mathcal{J} v + \eta (\mathcal{K} - \mathcal{L}) v + \alpha \Phi(v) v =: f(v). \quad (15)$$

In the following we show that the closed loop (15) can be interpreted as a distributed consensus protocol that aims to drive the relative phase shifts between the voltage vectors to the correct values while, at the same time, correcting their magnitude.

From Definition 2, we note that a solution to the power-flow equations characterized by consistent set-points p_k^* , q_k^* , v_k^* , $k = 1, \dots, N$ can be equivalently expressed by the voltage set-points v_k^* , $k = 1, \dots, N$ together with relative angle set-points. *w.l.o.g.* we consider relative angle set-points $\{\theta_{k1}^*\}_{k=2}^N$ with respect to the first inverter, which is taken as a reference and we define $\theta_{jk}^* := \theta_{j1}^* - \theta_{k1}^*$.

Proposition 1 (Interpretation of the controller)

The matrices K_k defined in (11) can be equivalently constructed in terms of relative-angle and voltage set-points as

$$K_k := \sum_{(j,k) \in \mathcal{E}} w_{jk} \left(I_2 - \frac{v_j^*}{v_k^*} R(\theta_{jk}^*) \right) \quad (16)$$

The proof is given in the Appendix.

We define the phase error $e_\theta := [e_{\theta,1}^\top \dots e_{\theta,N}^\top]^\top$ between each inverter and its interconnected inverters, with

$$e_{\theta,k} := \sum_{(j,k) \in \mathcal{E}} w_{jk} \left(v_j - \frac{v_j^*}{v_k^*} R(\theta_{jk}^*) v_k \right). \quad (17)$$

Given $v^* > 0$, let us define the voltage magnitude error $e_{v,k} := \Phi_k(v_k) v_k$ of inverter k and $e_v := \Phi(v) v$, with $\Phi(v)$ defined in (14).

Proposition 2 (Consensus-like dynamics)

The Closed-loop (15) can then be written as

$$\frac{d}{dt} v = \omega_0 \mathcal{J} v + \eta e_\theta + \alpha e_v. \quad (18)$$

Proof: We can write the phase error as

$$\begin{aligned} e_{\theta,k} &= \sum_{(j,k) \in \mathcal{E}} w_{jk} \left(v_j - \frac{v_j^*}{v_k^*} R(\theta_{jk}^*) v_k - v_k + v_k \right) \\ &= \sum_{(j,k) \in \mathcal{E}} w_{jk} (v_j - v_k) + K_k v_k, \end{aligned}$$

where the last equality follows from Proposition 1. Thus, $e_\theta = (\mathcal{K} - \mathcal{L})v$ and the proof is complete. ■

The first term in (18) makes sure that, at steady state, all voltage vectors rotate with frequency ω_0 , the second term regulates the relative angles θ_{jk} to the desired set-points θ_{jk}^* and the third term controls the voltage magnitude. Note that, if the phase angles and voltage magnitudes are correct, i.e., $e_\theta = e_v = 0$, the residual dynamics of (18) are those of N decoupled harmonic oscillators with synchronous frequency ω_0 . In Theorem 1 (Section V) we show that (18) indeed drives the system to synchrony and satisfies all objectives described in Section III from almost all initial conditions.

C. A dispatchable virtual oscillator

The closed loop (15), if analyzed in polar coordinates, is closely related to Virtual Oscillator Control (VOC) proposed in [13]. For ease of comparison we consider the case of purely resistive lines, i.e. $\kappa = 0$. Let us define $\theta_k := \tan^{-1} \left(\frac{v_{k\beta}}{v_{k\alpha}} \right)$,

Proposition 3 (Polar coordinates) *If $\ell_{jk} = 0$, $\forall (j,k) \in \mathcal{E}$, the closed loop (18) in polar coordinates is given by*

$$\begin{aligned} \dot{\theta}_k &= \omega_0 - \eta \left(\frac{q_k^*}{v_k^{*2}} - \frac{q_k}{\|v_k\|^2} \right), \\ \|\dot{v}_k\| &= \eta \left(\frac{p_k^*}{v_k^{*2}} - \frac{p_k}{\|v_k\|^2} \right) \|v_k\| + \alpha \left(\|v_k\| - \frac{1}{v_k^*} \|v_k\|^2 \right), \end{aligned} \quad (19)$$

where p_k and q_k are the active and reactive powers injected by the k^{th} inverter.

The proof is omitted for reasons of space. The averaged equations arising for VOC for a purely resistive grid [21], expressed in polar coordinates, are given by

$$\begin{aligned} \dot{\theta}_k &= \omega_0 + \eta \frac{q_k}{\|v_k\|^2}, \\ \|\dot{v}_k\| &= -\eta \frac{p_k}{\|v_k\|} + \alpha \left(\|v_k\| - \beta \|v_k\|^3 \right). \end{aligned} \quad (20)$$

Comparing (19) and (20) we note that the proposed control scheme leads to a closed-loop which is strikingly similar to VOC. However, unlike VOC, the controller (19) can receive power and voltage set-points p_k^* , q_k^* , v_k^* and thus synchronizes the power system to the desired power-flow solution and not the trivial solution where no power is flowing in the network.

Droop control is a proportional control strategy that trades off frequency and voltage magnitude deviations with active and reactive power imbalances. Unsurprisingly, much like VOC [12], [13], (19) resembles a droop controller around the normal operating point ($v_k \approx v_k^* = 1$). However, (19) differs greatly from a standard droop dynamics during large transients allowing, unlike droop controllers, to synchronize the grid from almost all initial conditions.

V. STABILITY ANALYSIS

We are now ready to state the main result of the paper. We begin by giving a geometric interpretation to the three control objectives presented in Section III, then, in Theorem 1, we show that under verifiable assumptions on the set-points and grid parameters, the voltages under the closed-loop dynamics (18) synchronize from almost all initial conditions.

A. Geometric re-formulation of the control objectives

Given a vector field f and $\omega_0 \geq 0$ we define the set

$$\mathcal{F}_{f,\omega_0} := \{v \in \mathbb{R}^n \mid f(v) - \omega_0 \mathcal{J}v = 0\},$$

Given $\{\theta_{k1}^*\}_{k=2}^N$, with $\theta_{k1} \in [-\pi, \pi]$ we define the set

$$\mathcal{S} := \left\{ v \in \mathbb{R}^n \mid \frac{v_k}{v_k^*} - R(\theta_{k1}^*) \frac{v_1}{v_1^*} = 0, k \in \mathcal{V} \setminus \{1\} \right\},$$

finally, given voltage magnitude set-points $v_k^* > 0$ let us define the set

$$\mathcal{A} := \{v \in \mathbb{R}^n \mid \|v_k\| = v_k^*, k \in \mathcal{V}\}.$$

Finally we define $\mathcal{T}_{f,\omega_0} := \mathcal{F}_{f,\omega_0} \cap \mathcal{S} \cap \mathcal{A}$.

The control objectives proposed in Section III are equivalent to requiring that, for the closed loop vector field f ,

- 1) The set \mathcal{T}_{f,ω_0} is stable under f .
- 2) The solutions $v(t)$ converge to \mathcal{T}_{f,ω_0} as $t \rightarrow \infty$.

Let us define the matrix whose span is the set \mathcal{S} as

$$S := \frac{1}{\sqrt{\sum_k v_k^{*2}}} \begin{bmatrix} v_1^* I \\ v_2^* R(\theta_{21}^*) \\ \vdots \\ v_N^* R(\theta_{N1}^*) \end{bmatrix},$$

and the matrix P as the projector onto the subspace orthogonal to \mathcal{S} as $P := I - SS^\top$.

Assumption 2 (Set-points and design parameters)

Let $T \in \mathbb{R}^{n \times (n-2)}$ be any matrix that spans \mathcal{S}^\perp , then the graph \mathcal{G} , the angle set-points $\{\theta_{k1}^*\}_{k=2}^N$, and the design parameters $\alpha > 0$ and $\eta > 0$ are such that

$$\eta T^\top [(\mathcal{K} - \mathcal{L})^\top P + P(\mathcal{K} - \mathcal{L})] T + 2\alpha T^\top P T \prec 0 \quad (21)$$

Assumption 2 can be verified with an LMI in α and η . With the following proposition we show that, regardless of the line parameters, if the power network is connected, for small enough angle set-points and uniform enough voltage set-points, Assumption 2 is satisfied.

Proposition 4 (Small angle set-point condition)

Let $v^* > 0$ be the nominal voltage magnitude. If the graph \mathcal{G} is connected, there exists non-empty open intervals \mathcal{I}_θ with $0 \in \mathcal{I}_\theta$ and \mathcal{I}_v with $v^* \in \mathcal{I}_v$ such that, for all $\theta_{k1}^* \in \mathcal{I}_\theta$ and $v_k^* \in \mathcal{I}_v$, there exists parameters $\alpha > 0$ and $\eta > 0$ such that Assumption 2 holds.

Proof: The entries of the matrix

$$Q_T := T^\top [(\mathcal{K} - \mathcal{L})^\top P + P(\mathcal{K} - \mathcal{L})] T$$

depend continuously on the vector of angle set-points θ^* . If $\theta^* = 0$ and $v_k^* = v^*$, then $\mathcal{K} = 0_{n \times n}$ and $\mathcal{LP} = \mathcal{L}$. Since the graph is connected, the second smallest eigenvalue of the Laplacian is strictly positive and we can conclude that

$$Q_T \Big|_{\substack{\theta_{k1}^* = 0 \\ v_k^* = v^*}} = -2T^\top \mathcal{L}T \prec 0.$$

The eigenvalues of a matrix are continuous with respect to its entries [22], therefore there exists non-empty open intervals \mathcal{I}_θ with $0 \in \mathcal{I}_\theta$ and \mathcal{I}_v with $v^* \in \mathcal{I}_v$, such that $Q_T \prec 0$ for all $\theta_{k1}^* \in \mathcal{I}_\theta$. If $\theta_{k1}^* \in \mathcal{I}_\theta$ and $v_k^* \in \mathcal{I}_v$, because all eigenvalues of Q_T are strictly smaller than zero, given $\eta > 0$ one can always pick $\alpha > 0$ small enough such that Assumption 2 holds. ■

By showing that for small angle set-points and uniform enough voltage set-points (21) always holds, Proposition 4 gives a theoretical justification to Assumption 2, which is satisfied in all practical examples we considered.

Theorem 1 (Almost global synchronization)

If the power set-points (p_k^*, q_k^*, v_k^*) are consistent according to Definition 2 and satisfy Assumption 2, the set $\mathcal{T}_{f, \omega_0}$ is almost globally asymptotically stable with respect to the dynamics (15).

The steps needed to prove Theorem 1 are the following. Under Assumption 2, we show that the set \mathcal{S} is exponentially stable. Therefore, the system converges exponentially to a state in which the voltage vectors have the correct relative angles and magnitude ratios. Moreover, the origin 0_n is an unstable equilibrium. We then show that, starting in $\mathcal{S} \setminus \{0_n\}$, the set \mathcal{A} is asymptotically stable. Hence the magnitudes of the voltage vectors converge to the desired set-points from $\mathcal{S} \setminus \{0_n\}$. Finally using a continuity argument inspired by [23], we prove that, from almost all initial conditions, the trajectories get steered towards \mathcal{A} as they approach \mathcal{S} . The full proof is lengthy and is beyond the scope of this paper. It will be presented in a further publication by the authors.

VI. POWER SYSTEMS TEST-CASE

In this section we demonstrate the decentralized synchronizing controller with a power systems test-case. We consider three inverters connected by a resistive-inductive grid as illustrated in Figure 2. The grid base power is 1 GW, the base voltage 320 kV and the base frequency 50 Hz. The line resistance is 0.03 Ohm/km and the line reactance is 0.3 Ohm/km (at the nominal frequency). Therefore, the reactance/resistance ratio ρ of the transmission lines is given by $\omega_0 \rho = 10$ and the angle κ can be computed as $\kappa = \tan^{-1}(10) = 84.2894^\circ$.

We simulate the following events

- **Black start at $t = 0$ s:** The grid is black started. Each inverter is given zero active and reactive power set-points $p_k^* = q_k^* = 0$ and voltage set-point $v_k^* = 1$. The inverters compute the matrices K_k according to (11) and implement the control laws (13)
- **Dispatch at $t = 5$ s:** We simulate a dispatch for the power-system. Each inverter is given power and voltage

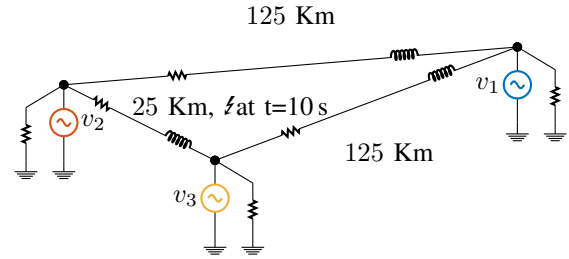


Fig. 2. Inverter based grid

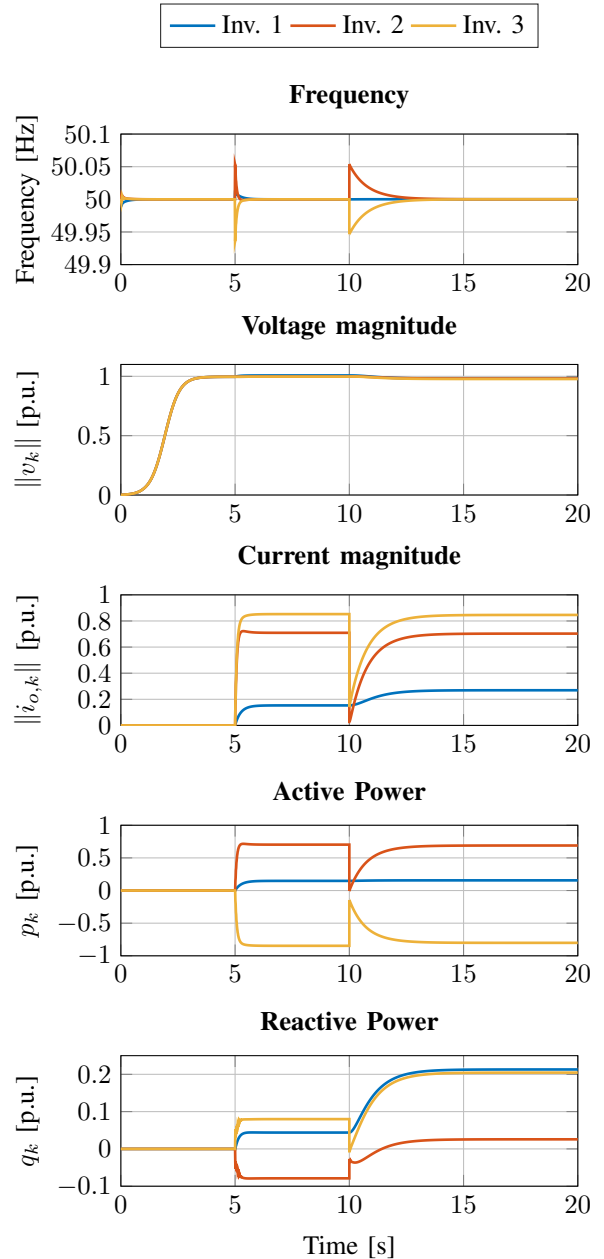


Fig. 3. The grid is black started then, at $t = 5$ s the inverters are dispatched to the set-points of Table I and at $t = 10$ s the transmission line connecting Inverters 2 and 3 is cut.

TABLE I

POWER AND VOLTAGE SET-POINTS FOR THE THREE INVERTERS

Power and voltage set-points			
Inverter k	p_k^* p.u.	q_k^* p.u.	v_k^* p.u.
Inverter 1	0.1458	0.0432	1.01
Inverter 2	0.7066	-0.0793	1
Inverter 3	-0.8509	0.0803	1

set-points as per Table I, and updates its controller matrix K_k according to (11). Note that Inverter 3 is controlled to draw active power thus simulating a load.

- **Contingency at $t = 10$ s:** The 25 Km line that connects Inverters 2 and 3 is cut. Note from Table I that Inverter 2 is producing most of the active power drawn by Inverter 3. This is therefore the most severe line failure for this setup as the power produced by Inverter 2 has to be diverted over 250 Km of transmission lines to reach Inverter 3.

Each inverter computes its control law according to (13) with the control gains $\eta = 0.0015$ and $\alpha = 0.015$. Assumption 2 can be easily verified. The simulation is performed including the dynamics of the transmission lines. From Figure 3 we notice that the controller is able to black-start the grid, converge to the desired set-points and ride through the severe contingency.

VII. CONCLUSION AND OUTLOOK

In this paper we propose a new decentralized control method for grid-connected power inverters that ensures synchronization and almost global convergence to a solution with the desired pre-specified power injections. This work opens to numerous further research directions. A question that arises naturally is the analysis of the proposed control method for the case of dynamic lines, inconsistent set-points, actively controlled loads that try to draw constant power and the presence of synchronous generators.

APPENDIX

Proof of Proposition 1: Since $\kappa = \tan^{-1}(\rho\omega_0)$, using the trigonometric identities $\sin(\kappa) = \frac{\ell_{jk}\omega_0}{\sqrt{r_{jk}^2 + \omega_0^2 \ell_{jk}^2}}$, and $\cos(\kappa) = \frac{r_{jk}}{\sqrt{r_{jk}^2 + \omega_0^2 \ell_{jk}^2}}$. we can write (7) as

$$\begin{aligned} p_k^* &= v_k^{*2} \sum_{(j,k) \in \mathcal{E}} w_{jk} \left[\cos(\kappa) - \frac{v_j^*}{v_k^*} \cos(\theta_{jk}^* - \kappa) \right], \\ q_k^* &= v_k^{*2} \sum_{(j,k) \in \mathcal{E}} w_{jk} \left[\sin(\kappa) + \frac{v_j^*}{v_k^*} \sin(\theta_{jk}^* - \kappa) \right]. \end{aligned} \quad (22)$$

From (22) we note that

$$\begin{bmatrix} p_k^* & q_k^* \\ -q_k^* & p_k^* \end{bmatrix} = v_k^{*2} R(\kappa)^\top \sum_{(j,k) \in \mathcal{E}} w_{jk} \left(I_2 - \frac{v_j^*}{v_k^*} R(\theta_{jk}^*) \right).$$

and (16) immediately follows from (11). ■

REFERENCES

- [1] Q.-C. Zhong and G. Weiss, "Synchronverters: Inverters that mimic synchronous generators," *IEEE Transactions on Industrial Electronics*, vol. 58, no. 4, pp. 1259–1267, 2011.
- [2] T. Jouini, C. Arghir, and F. Dörfler, "Grid-friendly matching of synchronous machines by tapping into the DC storage," in *IFAC Workshop on Distributed Estimation and Control in Networked Systems*, 2016, pp. 192–197.
- [3] S. D'Arco and J. A. Suul, "Virtual synchronous machines—Classification of implementations and analysis of equivalence to droop controllers for microgrids," *IEEE PowerTech*, 2013.
- [4] G. Denis, T. Prevost, P. Panciatici, X. Kestelyn, F. Colas, and X. Guillaud, "Review on potential strategies for transmission grid operations based on power electronics interfaced voltage sources," in *IEEE Power Energy Society General Meeting*, 2015.
- [5] H. Bevrani, T. Ise, and Y. Miura, "Virtual synchronous generators: A survey and new perspectives," *International Journal of Electrical Power and Energy Systems*, vol. 54, no. C, pp. 244–254, Jan. 2014.
- [6] M. C. Chandorkar, D. M. Divan, and R. Adapa, "Control of parallel connected inverters in standalone AC supply systems," *IEEE Transactions on Industry Applications*, vol. 29, no. 1, pp. 136–143, 1993.
- [7] J. M. Guerrero, M. Chandorkar, T.-L. Lee, and P. Chiang Loh, "Advanced control architectures for intelligent microgrids — Part I: Decentralized and hierarchical control," *IEEE Transactions on Industrial Electronics*, vol. 60, no. 4, pp. 1254–1262, 2013.
- [8] J. W. Simpson-Porco, F. Dörfler, and F. Bullo, "Synchronization and power sharing for droop-controlled inverters in islanded microgrids," *Automatica*, vol. 49, no. 9, pp. 2603–2611, 2013.
- [9] F. Dörfler, M. Chertkov, and F. Bullo, "Synchronization in complex oscillator networks and smart grids," *Proceedings of the National Academy of Sciences*, vol. 110, no. 6, pp. 2005–2010, 2013.
- [10] F. Dörfler and F. Bullo, "Synchronization and transient stability in power networks and nonuniform Kuramoto oscillators," *SIAM Journal on Control and Optimization*, vol. 50, no. 3, pp. 1616–1642, 2012.
- [11] B. B. Johnson, S. V. Dhople, A. O. Hamadeh, and P. T. Krein, "Synchronization of parallel single-phase inverters with virtual oscillator control," *IEEE Transactions on Power Electronics*, vol. 29, no. 11, pp. 6124–6138, 2014.
- [12] J. W. Simpson-Porco, F. Dörfler, and F. Bullo, "Voltage stabilization in microgrids via quadratic droop control," *IEEE Transactions on Automatic Control*, vol. 62, no. 3, pp. 1239–1253, 2017.
- [13] M. Sinha, F. Dörfler, B. Johnson, and S. Dhople, "Uncovering droop control laws embedded within the nonlinear dynamics of van der pol oscillators," *IEEE Transactions on Control of Network Systems*, vol. 4, no. 2, pp. 347–358, 2017.
- [14] M. Sinha, F. Dörfler, B. B. Johnson, and S. V. Dhople, "Synchronization of Liénard-type oscillators in uniform electrical networks," in *American Control Conference*, 2016, pp. 4311–4316.
- [15] L. Törres, J. Hespanha, and J. Moehlis, "Synchronization of oscillators coupled through a network with dynamics: A constructive approach with applications to the parallel operation of voltage power supplies," September 2013, submitted.
- [16] B. B. Johnson, M. Sinha, N. G. Ainsworth, F. Dörfler, and S. V. Dhople, "Synthesizing virtual oscillators to control islanded inverters," *IEEE Transactions on Power Electronics*, vol. 31, no. 8, pp. 6002–6015, 2016.
- [17] J. N. Tsitsiklis, "Problems in decentralized decision making and computation." MIT Laboratory for Information and Decision Systems, Tech. Rep., 1984.
- [18] F. Bullo, *Lectures on Network Systems*. Version 0.95, 2017, with contributions by J. Cortes, F. Dörfler, and S. Martinez. [Online]. Available: <http://motion.me.ucsb.edu/book-lns>
- [19] E. Clarke, *Circuit analysis of AC power systems*. Wiley, 1943, vol. 1.
- [20] P. Kundur, *Power system stability and control*. McGraw-hill, 1994.
- [21] B. Johnson, M. Rodriguez, M. Sinha, and S. Dhople, "Comparison of virtual oscillator and droop control," in *IEEE Workshop on Control and Modeling for Power Electronics*, 2017.
- [22] R. A. Horn and C. R. Johnson, *Matrix analysis*. Cambridge university press, 1985.
- [23] E. D. Sontag, "A remark on the converging-input converging-state property," *IEEE Transactions on Automatic Control*, vol. 48, no. 2, pp. 313–314, Feb 2003.